Observations on the Behavior of Surface Flaws in the Presence of Cladding*

S. K. ISKANDER and R. K. NANSTAD
Metals and Ceramics Division, Oak Ridge National Laboratory, P. O. Box 2008, Bldg. 4500S, MS 6151, Oak Ridge, TN 37831-6151, USA

ABSTRACT

A small crack near the inner surface of clad nuclear reactor pressure vessels (RPV) is an important consideration in the safety assessment of the structural integrity of the vessel. Four-point bend tests on large plate specimens, six clad and two unclad, were performed to determine the effect, if any, of stainless steel cladding upon the propagation of small surface cracks subjected to stress states similar to those produced by pressurized thermal shock conditions. Results of tests at temperatures 10 and 60°C below the nil-ductility-transition temperature (NDT) have shown that (1) a tough surface layer composed of cladding and/or heat-affected zone has arrested running flaws in clad plates under conditions where unclad plates have ruptured, and (2) the residual load-bearing capacity of clad plates with large subclad flaws significantly exceeded that of an unclad plate.

KEYWORDS

Surface flaws; reactor pressure vessels; cladding; pressurized thermal shock; heat-affected zone; fracture mechanics; crack arrest; crack initiation; finite length flaws.

---

*Research sponsored by the Office of Nuclear Regulatory Research, Division of Engineering, U.S. Nuclear Regulatory Commission under Interagency Agreement DOE 1886-8011-9B with the U.S. Department of Energy under contract DE-AC05-84OR21400 with Martin Marietta Energy Systems, Inc.

NOMENCLATURE

Acronyms

CP-*n*	Clad plate number *n*
CVN	Charpy V-notch
EB	Electron beam
HAZ	Heat-affected zone
NDT	Nil-ductility-transition temperature, as determined by the drop-weight test according to ASTM E 208
ORNL	Oak Ridge National Laboratory
PTS	Pressurized thermal shock
RPV	Reactor pressure vessel
TSE-*n*	Thermal shock experiment *n*

Symbols

K_I	Plain strain stress intensity factor
b/a	Ratio of major to minor axes length of elliptical flaw, see Fig. 1.

INTRODUCTION

There are considerable experimental results which have shown that, *in the absence of cladding*, a small surface flaw in an embrittled material subjected to severe thermal shock will become a long flaw (Iskander, 1986). However, the questions remain about the role a tough surface cladding will play in preventing the propagation of small flaws along the surface. Furthermore, the flaw could tunnel beneath the cladding, in which case the residual strength of the structure needs to be estimated. The question is of more than academic interest, since a small crack near the inner surface of clad nuclear reactor pressure vessels (RPV) is an important consideration in the safety assessment of the structural integrity of the vessel. The behavior of such flaws is relevant to the pressurized thermal shock (PTS) scenario and to the plant life extension issue.

There is a dearth of information on the behavior of small flaws in the presence of cladding. This has led at least one RPV integrity study (Iskander, 1986) to assume infinitely long flaws (although small flaws are certainly more credible). To date, it is difficult to predict the behavior of finite length flaws for various reasons. An important one is that no criteria exist to predict the evolution of the flaw geometry thus, only general qualitative estimates can be made in such terms as "there is a tendency for the crack to propagate along the surface." Another important reason is the analytical complexity introduced by the three-dimensional nature of finite length flaws. Figure 1 shows the variation of the stress intensity factor K_I for an elliptical flaw as a function of the aspect ratio of the major to minor axes (b/a) for the conditions pertaining to the TSE-7 experiment (Cheverton et al., 1985). These curves show that for the initial 19-mm radius semicircular surface flaw used (b/a = 1), the stress intensity factor at the bottom of the flaw is less than that at the surface until b/a exceeds 3. Thus, such a flaw has a tendency to initiate and propagate on the surface to some extent before it can increase in depth. This has indeed been verified experimentally, Fig. 2, which shows the extensive propagation and bifurcation on the surface of the TSE-7 cylinder originating from the semicircular surface flaw. The flaw also increased in depth to the values shown at many selected locations in Fig. 2. It is now an article of faith in the Oak Ridge National Laboratory's (ORNL) Heavy Section Steel Technology program that, in the absence of cladding, a short flaw will grow to become a long one.

The central question to be investigated is whether a relatively thin layer of tough cladding by maintaining its integrity can redistribute the stresses in its immediate vicinity sufficiently to retard crack propagation that would have otherwise occurred. In particular, could cladding arrest an initially short flaw that is propagating along the surface and keep it from becoming a long flaw? Should that occur, then the flaw cannot grow in depth to challenge the integrity of the plate without a significant increase of load beyond that needed to rupture unclad plates. A clad plate research program was conducted as part of ORNL's Heavy Section Steel Technology program in order to investigate the behavior of small flaws in the presence of cladding. The objectives of this research were achieved by comparing the load-bearing capacity of clad and unclad flawed plates.

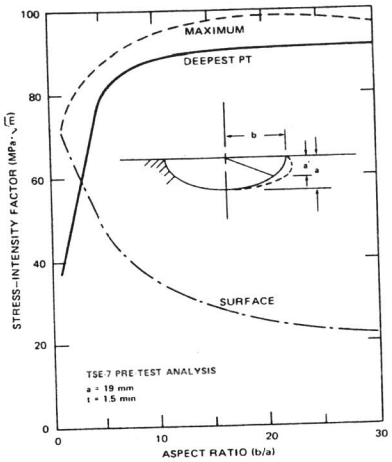

Fig. 1. Variation of the stress intensity factor K_I for an elliptical flaw as a function of the aspect ratio of the major to minor axes (b/a) (Cheverton et al., 1985).

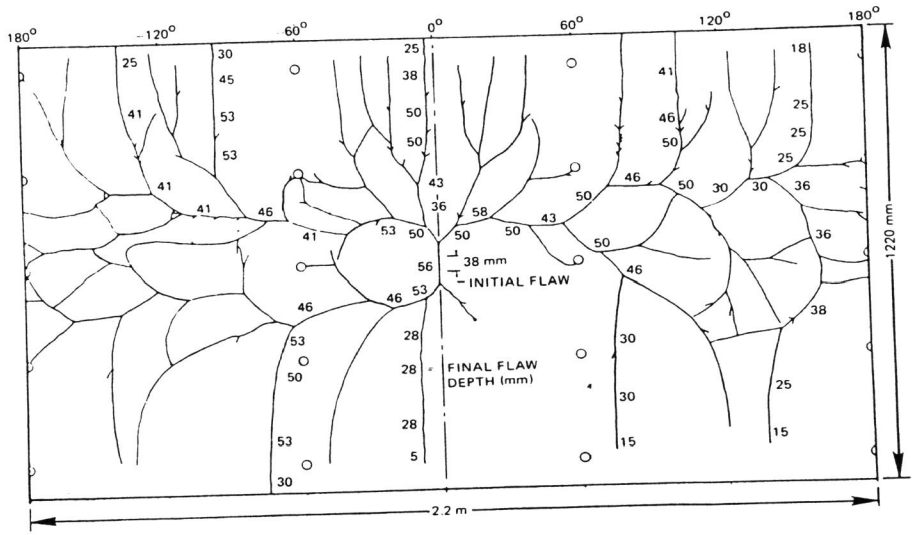

Fig. 2. Developed view of inner surface of the TSE-7 cylinder in which the 19-mm radius semicircular flaw propagated on the surface to become a long flaw during the test (Cheverton et al., 1985).

EXPERIMENTAL PROGRAM

A special plate specimen made of a typical RPV steel conforming to ASTM Specification for Pressure Vessel Plates, Alloy Steels, Quenched and Tempered, Manganese-Molybdenum and Manganese-Molybdenum-Nickel (A 533) Grade B, has been developed to investigate the effects of cladding on the behavior of flaws, Fig. 3. It was commercially clad using the three-wire series-arc technique and stainless steel type 308, 309, and 312 weld wires. The three-wire series-arc technique was used in some of the older vessels. An electron-beam (EB) weld is introduced into the base metal to provide a crack initiation site. At the time a sharp flaw is required, the EB-weld site is hydrogen charged (Holz, 1980). The plate is loaded in four-point bending to approximate the stresses due to PTS.

To initiate a flaw, six initially unflawed plates were hydrogen charged while the load was maintained constant. This test will be termed an "arrest" type, and its purpose was to determine the arrest capacity of clad plates under various amounts of stored energy. In tests on two plates, the flaw was initiated through hydrogen charging before the plate was loaded, which will be termed "initiation" tests. The purpose of initiation experiments was to determine the load-carrying capacity of flawed plates. The flaw, once it initiated from the EB-weld region, either arrested or lead to complete rupture of the plate. Plates which did not rupture were heat-tinted to define the arrested flaw shape and were then reloaded until either another pop-in or plate rupture occurred.

Arrest Type Experiments

The target surface strains and corresponding, loads for the six plates tested are given in Table 1. For applicable cases the load that the specimen can support after pop-in, the "arrest" load, is also given. The surface strain (in the uniform bending moment span of the plate) was the independent parameter used in the selection of the target load. All arrest experiments were performed at either -25 or 25°C, and Fig. 4 shows the point on the load vs surface strain curve at which the six plates have been tested. Plate designations shown on the left-hand side of the curve were tested at -25°C, and those on the right-hand side were tested at 25°C. The loads (and strains) were maintained constant under stroke control during the period of hydrogen charging and are a measure of the crack driving force acting (or the potential energy stored in the plate) during the instant the flaw initiated in the EB weld.

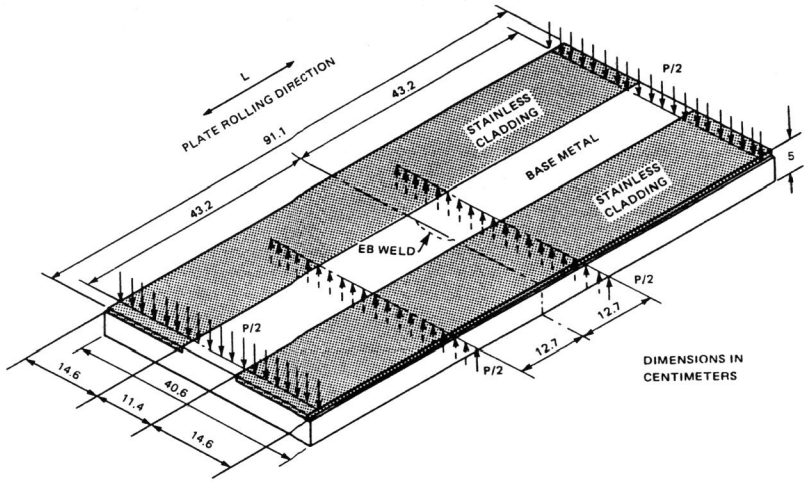

Fig. 3. Clad plate specimen.

Table 1. Target surface strains and corresponding loads for the six plates tested

Plate	Condition	Test temperature[a] (°C)	Load (kN)		Target surface strain (%)
			Pop-in	Arrest[b]	
CP-15	Clad	RT	676	654	0.31
		-25	759	709	
		-100	600	R	
CP-17	Clad	RT	890	823	0.45
	Several pop-ins occurred before rupture	-25	756/725	R	
CP-19	Clad	RT	987	689	0.65
		-50	703	R	
CP-21	Unclad	RT	676	R	0.27
CP-18	Clad	-25	823	649	0.39
		-25	698	R	
CP-20	Clad	-25	868	R	0.41

[a] RT - room temperature, approximately 25°C.

[b] R - plate ruptured in two pieces.

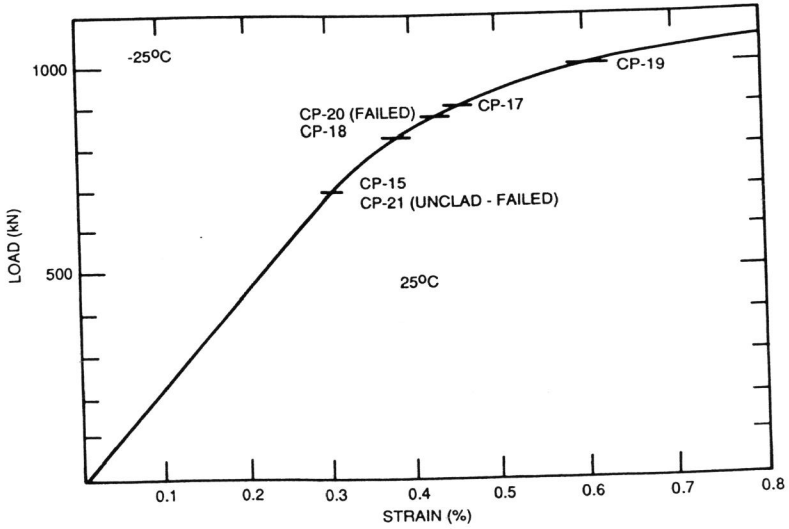

Fig. 4. Point on load vs surface strain curve at which the six plates were tested in the "arrest" mode. Note that all plates whose designations appear above the curve were tested at -25°C, while those below the curve were tested at 25°C.

For the first clad plate tested, CP-15, the surface strain was chosen to be approximately the yield strain of the base metal. The plate did not rupture. The target surface strain was increased for plates CP-17 and CP-19. In all three cases the flaw initiated and arrested after propagating beneath the cladding a distance that increased with increasing target strain. An unclad plate, CP-21, ruptured when loaded to approximately the base metal yield strain on the surface. The pop-in, arrest loads, and corresponding crack lengths for the four plates tested at room temperature are shown schematically in Fig. 5. It may be noted that as the potential energy stored in the plate increased, the length of the arrested flaw also increased, as shown schematically by the shaded flaw shape in Fig. 5. Photographs of actual fracture surfaces of the plates are shown in Fig. 6. From these photographs it may be noted that in almost all cases a surface layer composed of heat-affected zone (HAZ) and cladding arrested the flaw and prevented its propagation along the surface, caused it to tunnel below the surface. Full details can be found in an earlier presentation (Iskander, 1988a).

The remaining two clad plates, CP-18 and CP-20, were tested at -25°C in order to bracket another point besides room temperature on an arrest vs temperature curve for the plates. As may be seen in Table 1, the arrest load for clad plate CP-18 is just 4% lower than the load that ruptured unclad plate CP-21, even though the temperature was some 50 K lower. Moreover, the rupture load of clad plate CP-20 at -25°C is only 5% higher than the corresponding pop-in load (that lead to arrest) for clad plate CP-18. Thus, it can be assumed that the load-arresting capacity of the cladding for these plates at -25°C is approximately 800 kN.

Initiation Type Tests on Plates CP-16 and CP-22

The loads at various events for clad plate CP-16 and unclad plate CP-22 are shown in Table 2. Recalling that these two plates were tested with pre-existing flaws, it is interesting to noted that the pop-in load for plate CP-16 is within 5% of the target load (chosen on the basis of the yield on surface of base metal) for the "arrest" test unflawed plate CP-15. The arrested crack shapes also are very similar. Almost the same loads have lead to rupture in both the unclad plates tested. The fracture surfaces of these two plates are very similar to those from arrest experiments, and have been presented elsewhere (Iskander, 1988b).

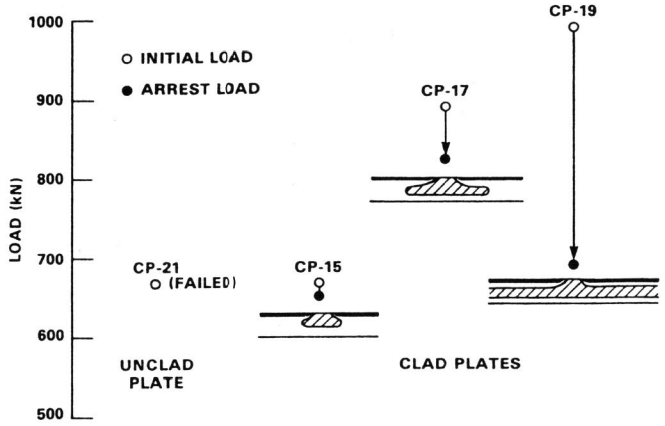

Fig. 5. Pop-in, arrest loads, and corresponding crack lengths for the four plates tested at room temperature.

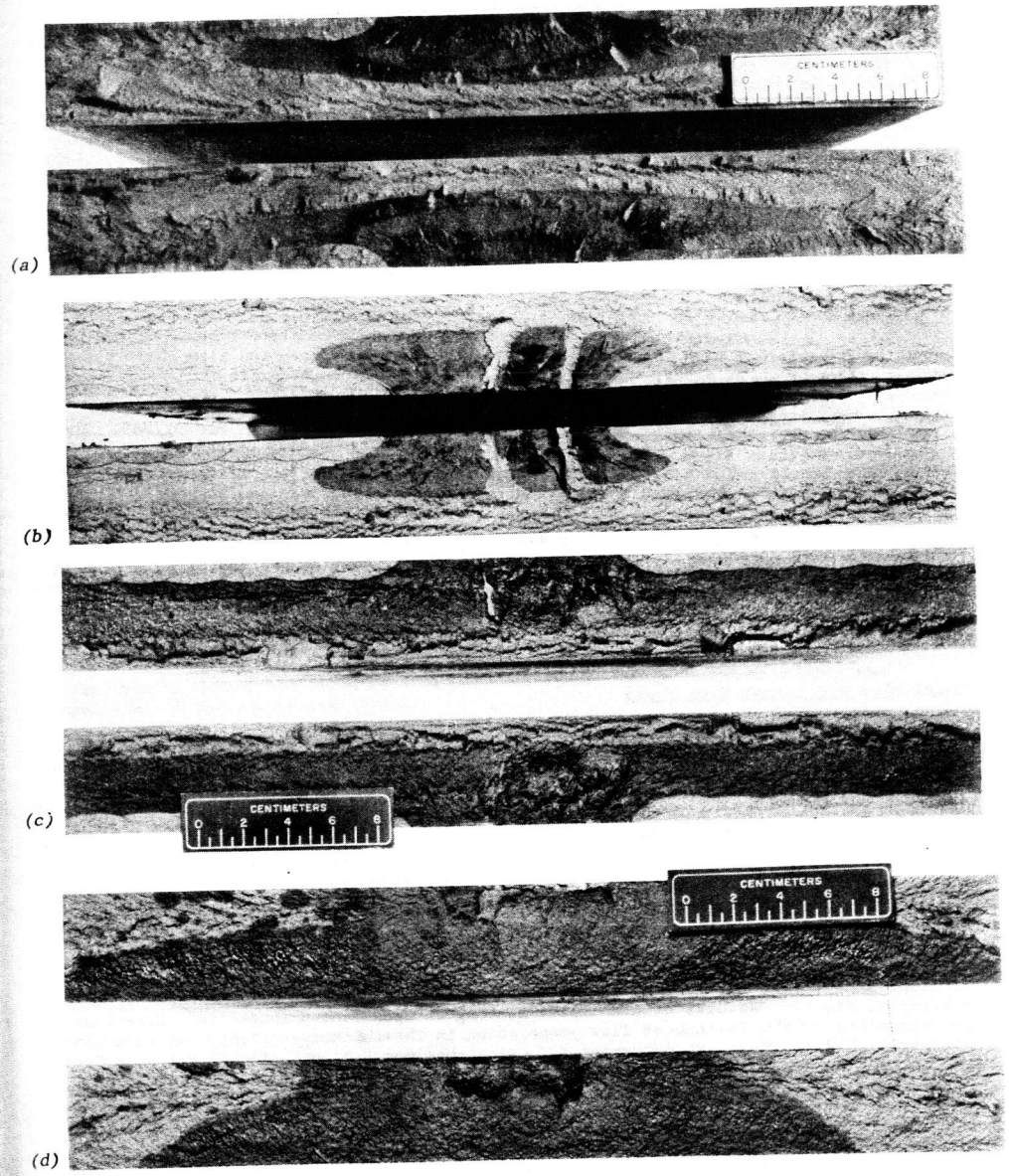

Fig. 6. Fracture surfaces from top to bottom of clad plates (*a*) CP-15, (*b*) CP-17, (*c*) CP-19 and (*d*) unclad plate CP-21.

Table 2. Summary of initiation and arrest loads for plates CP-16 and -22

Plate	Condition	Test temperature (°C)	Load (kN)	
			Pop-in	Arrest
CP-16	Clad	21	703	694
		21	890	738
		-25	698	Rupture
CP-22	Unclad	21	698	Rupture

RESULTS

Tunneling Behavior of Finite Length Surface Flaws

Examination of the fracture surfaces suspects a propensity for propagating flaws to tunnel, even without the aid of the tough surface layer composed of cladding/HAZ, The differing "textures" of the fracture surface of both unclad plates tested seem to indicate that the crack front first propagates below the surface, leaving a sharp pointed wedge-shaped unbroken ligament between the flaw and the surface. This ligament then cleaves when the stresses in it become sufficiently high thus re-establishing a through-crack, approximately elliptically shaped flaw configuration. The crack front propagates again below the surface, and the process repeats. This sequence of events appeared to have occurred in both unclad plates CP-21 and CP-22. This potential for tunneling is due to the location of the maximum stress intensity factor K_I for short flaws occurring somewhat below the surface when the flaw is in a stress gradient as in these tests. As an example, Fig. 1 shows that the location of the maximum K_I is neither at the surface nor at the deepest point of the flaw (Cheverton et al., 1985).

Initiation and Arrest Type Tests

The tough surface layer of cladding and HAZ seemed to have contributed significantly to the load-bearing capacity of the plates by arresting flaws at loads and temperatures that have ruptured unclad plates, as seen by comparing the results of the tests on plates CP-15 and CP-21. In fact, the clad plate CP-19 arrested a flaw subjected to a driving force (as measured by the target load) almost 50% higher than that which broke an unclad plate. Moreover, the residual load-bearing capacity of plates, as measured by the critical loads in initiation experiments with fairly large flaws, was generally greater than required to break the unclad plate, even though the test temperatures were lower by 50°C.

The HAZ played a prominent role in enhancing the load-carrying capacity of the clad plates. As measured by the Charpy V-notch (CVN) impact energy, the HAZ is the toughest of the three metallurgical zones of the clad plate specimens. CVN impact energy tests were performed on the cladding, HAZ, and base metal with specimens oriented in a direction corresponding to the EB-induced flaw propagating along the surface of the clad-plate specimens, Fig. 7. Results of CVN impact testing on specimens oriented in a direction corresponding to the EB-induced flaw propagating in the thickness orientation were similar (Iskander, 1987). Tests to determine NDT using specimen P-3 according to the ASTM Test for Conducting Drop-Weight Test to Determine Nil-Ductility Transition Temperature of Ferritic Steels (E 208) were also performed and have resulted in an NDT of 36°C. The results show that the cladding has a substantially lower ductile-to-brittle transition temperature than base metal as measured by the Charpy impact energy.

The Charpy transition of the HAZ is also noticeably lower than that of the bulk of the base metal. This is principally the result of the special heat treatment given to the base metal to raise its transition temperature. The base plate was first normalized at 1032°C for 2 h and air cooled. This produced a basically bainitic microstructure with a

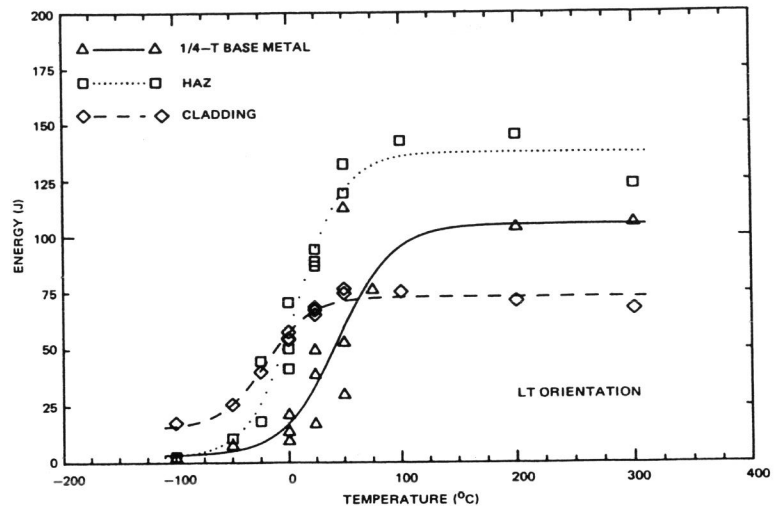

Fig. 7. Charpy impact energy of base metal, HAZ, and cladding used in the clad plates. Specimen orientation corresponds to EB-induced flaw propagating along the surface.

larger grain size than would be typical of a normally quenched and tempered A533B class 1 steel. This microstructure was needed to achieve a high transition temperature. The plate was then clad and given the milder-than-usual postweld heat treatment of 10 h at 593°C which tempered it only slightly. By comparison, material in the HAZ was transformed to martensite during the first welding pass and subsequently tempered during the deposition of the successive layers.

The residual load-bearing capacity of flawed plates, as measured by the critical loads during tests of clad plate specimens with fairly large flaws, was generally greater than that required to break unclad plates, Fig. 5, and Tables 1 and 2. Unclad plate CP-21 was loaded to 676 kN, and a running flaw was triggered by hydrogen charging. No arrest occurred; whereas, the flawed and unclad plate CP-22 ruptured at a load of 689 kN. Thus, the loads prior to fracture in both unclad plates differ by 2%. Allowing for scatter and the differences in the EB flaws, the small difference in loads for both plates indicates that dynamic effects for CP-21 must have been small.

It is not clear at this time whether cladding alone, without benefit of the tough HAZ which played a pronounced role in arresting propagating flaws, would have also elevated the load-bearing capacity. In the case of radiation-embrittled reactor pressure vessels, the HAZ will most likely undergo toughness degradation similar to that of the base metal, and would therefore not play such a prominent role in arresting propagating flaws.

REFERENCES

Cheverton, R. D., D. G. Ball, S. E. Bolt, S. K. Iskander, and R. K. Nanstad (1985). *Pressure Vessel Fracture Studies Pertaining to the PWR Thermal-Shock Issue: Experiment TSE-7*, NUREG/CR-4304 (ORNL-6177), Oak Ridge National Laboratory.

Holz, P. P. (1980). *Flaw Preparations for HSST Program Vessel Fracture Mechanics Testing: Mechanical Cyclic Pumping and Electron Beam Weld-Hydrogen-Charge Cracking Schemes*, NUREG/CR-1274 (ORNL/NUREG/TM-369), Oak Ridge National Laboratory.

Iskander, S. K. (1986). "A Method of LEFM Analysis of RPV During SBLOCA," *Int. J. Pressure Vessels Piping 25*, 279-298.

Iskander, S. K., et al. (1987). "Crack Arrest Behavior in Clad Plates," pp. 169-73 in *Heavy-Section Steel Technology Program Semiann. Prog. Rep. October 1986-March 1987*, NUREG/CR-4219, Vol. 4, No. 1 (ORNL/TM-9593/V4&N1), Oak Ridge National Laboratory.

Iskander, S. K., et al. (1988a). "Crack Arrest Behavior in Clad Plates," pp. 222-242 in *Heavy-Section Steel Technology Program Semiann. Prog. Rep. April-September 1987*, NUREG/CR-4219, Vol. 4, No. 2 (ORNL/TM-9593/V4&N2), Oak Ridge National Laboratory.

Iskander, S. K., et al. (1988b). "Crack Arrest Behavior in Clad Plates," pp. 212-226 in *Heavy-Section Steel Technology Program Semiann. Prog. Rep. October 1987-March 1988*, NUREG/CR-4219, Vol. 5, No. 1 (ORNL/TM-9593/V5&N1), Oak Ridge National Laboratory.